Title

Evaluating 225Ac and 177Lu Radioimmunoconjugates against Antibody—Drug Conjugates for Small-Cell Lung Cancer

Journal

Molecular Pharmaceutics, 17(11)

ISSN

1543-8384

Authors

Lakes, Andrew L

An, Dahlia D

Gauny, Stacey S

et al.

Publication Date

2020-11-02

DOI

10.1021/acs.molpharmaceut.0c00703

Peer reviewed

Research Article

Evaluating ^{225}Ac and ^{177}Lu Radioimmunoconjugates against Antibody-drug Conjugates for Small Cell Lung Cancer

Andrew L. Lakes [1], Dahlia D. An [1], Stacey S. Gauny [1], Camille Ansoborlo [1], Benjamin H. Liang [1], Julian A. Rees [1], Kristen D. McKnight [2], Holger Karsunky [2], Rebecca J. Abergel [1,3,*]

[1] Chemical Sciences Division, Lawrence Berkeley National Laboratory, Berkeley, CA 94720

[2] AbbVie-Stemcentrx, South San Francisco, CA 94080

[3] Department of Nuclear Engineering, University of California Berkeley, Berkeley, CA 94709

Corresponding author: Rebecca J. Abergel. rjabergel@lbl.gov.

Keywords: Radioimmunoconjugate, ^{225}Actinium, ^{177}Lutetium, Antibody Drug Conjugate, Small Cell Lung Cancer

TOC Graphic

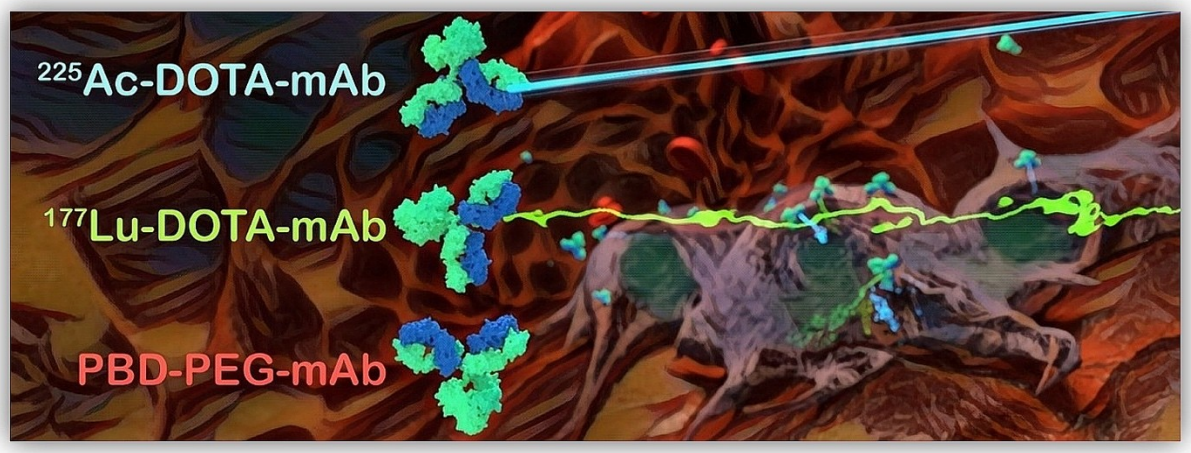

ABSTRACT

Interest in the use of ^{225}Ac for targeted alpha therapies has increased dramatically over the past few years, resulting in a multitude of new isotope production and translational research efforts. However, ^{225}Ac radioimmunoconjugate (RIC) research is still in its infancy, with most prior experience in hematologic malignancies and only one reported pre-clinical solid tumor study using ^{225}Ac RICs. In an effort to compare ^{225}Ac RICs to other current antibody-conjugates, a variety of RICs are tested against intractable small cell Lung cancer (SCLC). We directly compare, *in vitro* and *in vivo*, two promising candidates of each α or β^- category, ^{225}Ac and ^{177}Lu, vs pyrrolobenzodiazepine (PBD) non-radioactive benchmarks. The monoclonal antibody constructs are targeted to either delta like 3 protein (DLL3), a recently discovered SCLC target, or CD46 as a positive control. An immunocompromised maximum tolerated dose (MTD) assay is performed on NOD SCID mice, along with tumor efficacy proof-of-concept studies *in vivo*. We overview the conjugation techniques required to create serum-stable RICs, and characterize and compare *in vitro* cell killing with RICs conjugated to non-specific antibodies (huIgG1) with either native or site-specific thiol loci against tumor antigen DLL3-expressing and non-expressing cell lines. Using patient derived xenografts (PDX) of SCLC onto NOD SCID mice, solid tumor growth was controlled throughout 3 weeks before growth appeared, in comparison to PBD conjugate controls. NOD SCID mice showed lengthened survival using ^{225}Ac compared to ^{177}Lu RICs, and PBD dimers showed full tumor suppression with nine out of ten mice. The exploration of RICs on a variety of antibody-antigen systems is necessary to direct efforts in cancer research towards promising candidates. However, the anti-DLL3-RIC system with ^{225}Ac and ^{177}Lu appears to be not as effective as the anti-DLL3-ADC counterpart in SCLC therapy

with matched antibodies, and portrays the challenges in both SCLC therapy as well as the specialized utility of RICs in cancer treatment.

INTRODUCTION

With a 6.4% 5-year relative survival rate, small cell lung carcinomas (SCLC) continue to be an intractable and deadly public health problem (*1*,*2*). To assist in filling this health gap, AbbVie-Stemcentrx has developed an antibody drug conjugate (ADC), Rovalpituzumab tesirine (Rova-T). Rova-T targets delta-like protein 3 (DLL3), an inhibitory Notch receptor ligand expressed in neuroendocrine lung tumors, including SCLC, in greater than 80% of SCLC patients (*3*). Even though DLL3 expression is relatively low at the cell surface, DLL3 has been shown to be a highly selective target for immunotherapy due to its absence on non-malignant cells (*4*,*5*). While several ongoing clinical trials utilizing Rova-T formulations against SCLC have been halted due to low treatment efficacy, in an orthogonal approach to Rova-T's small molecule pyrrolobenzodiazepine (PBD) dimer payload, we aimed to formulate radioimmunoconjugates (RICs), utilizing α (^{225}Ac) and β$^-$ emitting (^{177}Lu) radionuclides attached to similar anti-DLL3 antibodies through a chelating linker based on the macrocyclic 1,4,7,10-Tetraazacyclododecane-1,4,7-tris-acetic acid-10-maleimidoethylacetamide (DOTA-MMA) scaffold, as depicted in **Figure 1**. These RICs were then compared directly against small molecule ADC analogs to Rova-T, with matched monoclonal antibodies.

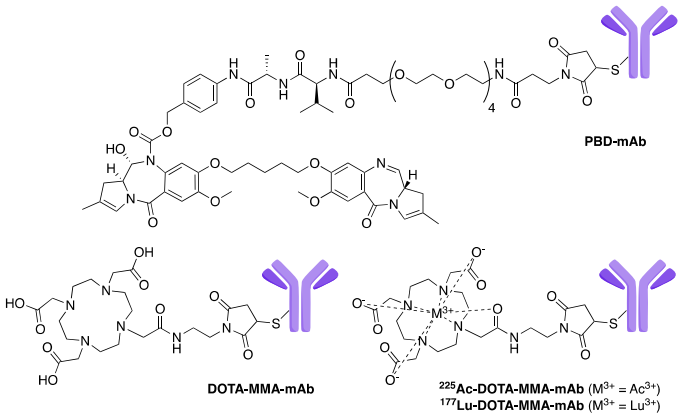

Figure 1. Molecular structures of PBD-carrying antibody drug conjugates and DOTA-MMA RICs (labeled with ^{225}Ac or ^{177}Lu) discussed in this study.

RICs may offer several benefits compared to small molecule ADCs. For instance, α and β^- emitting RICs do not require cellular internalization to display efficacy. This is due to their decay sphere of penetration being relatively larger than the cellular diameter, in comparison to small molecules that require Van der Waals radius distances to their drug target. Further, for RICs, radioisotopic/drug release may not be advantageous (*6*), and thus non-cleavable chelate linkers are often utilized in research, offering greater construct serum circulatory stability. Currently, payload cleavage is required for three of the four approved ADCs to be effective. These include DNA minor groove crosslinkers such as ozogamicin, the calicheamicin compound in Gemtuzumab ozogamicin and recently Inotuzumab ozogamicin, as well as antimitotic tubulin binders such as monomethyl auristatin E found in Brentuximab vedotin (*7*). However, Trastuzumab emtansine has a stable linker and requires intracellular catabolism to release the tubulin-binding maleimide-conjugated mertansine (DM1) (*7*). Nonetheless, less heavily-studied isotopes, such as ^{225}Ac, produce challenging chemistry in chelator design (*8*,*9*). Due to this, serum stability of conjugated DOTA complexes *in vivo* is still difficult to match to smaller, more studied isotopes such as ^{177}Lu, of which DOTA-MMA produces a superior ligand-metal complex compared to ^{225}Ac-DOTA-MMA.

While Zevalin (^{90}Y) and the formerly available Bexxar (^{131}I) both use β^- emitters, α emitters have displayed increasing momentum in research. α therapies have been on the market for some time in the non-immunotargeting format, as in ^{223}Ra

chloride (Xofigo) for bone metastases, and several elements with parent and/or daughter α decay, such as ^{227}Th, ^{225}Ac, $^{213/212}$Bi, and ^{211}At, are at various clinical stages as targeted constructs (*10*,*11*). Particular to this work, ^{225}Ac was of interest due to its potent daughter chain, creating four α particles and two β^- emissions over a half-life of 9.95 days for the parent ^{225}Ac, and a more rapid 50.45 minutes to complete all daughter α decays. With a power maximum reached after 13.4 hours, the ^{225}Ac chain produces 5.9 times the total counts per minute (CPM) of all daughter species, and 4.8 times the power starting from pure ^{225}Ac (see **Figure 2A**).

^{177}Lu has also been of research interest in somatostatin (Lutathera/DOTA-TATE) and prostate-specific membrane antigen (PSMA) targeted therapies for some time due to a favorable half-life (6.7 days) (see **Figure 2B**) and short range potency (*12*). Being a lower energy β^- emitter, ^{177}Lu has a shorter range than other high energy β^- emitters, such as ^{90}Y, making comparison of ^{225}Ac to ^{177}Lu of relevance to this work. Both ^{225}Ac and ^{177}Lu show *in vitro* and *in vivo* efficacy, but with a large difference in relative biological effectiveness (RBE), at roughly 5:1 ^{225}Ac:^{177}Lu (*13*).

RICs with various radioisotopes and ADCs with their various payload systems each have their pros and cons, and each of their uses is likely highly target and pathophysiologically dependent. In this work, we aimed to develop and determine if the targeted ^{225}Ac and/or ^{177}Lu RICs against DLL3 were more effective than PBD ADCs *in vitro* and *in vivo*.

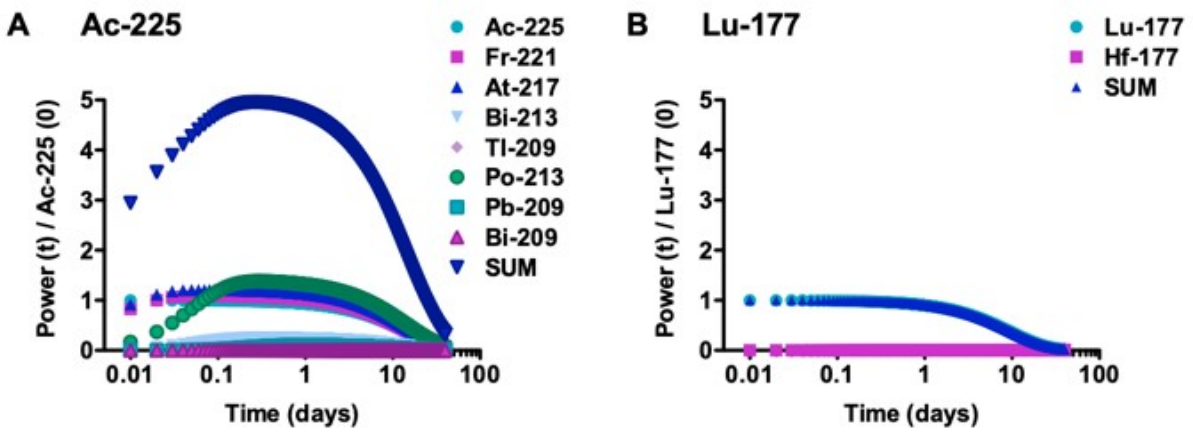

Figure 2. Percent power of species(i) at time(t) / parent isotope at time(0), where time(0) is the time of LSC counting, starting at equilibrium levels of 0.05 days from pure ^{225}Ac. **A**) ^{225}Ac and daughters, where 'sum' is the total power of all species. **B**) ^{177}Lu decay into ^{177}Hf.

MATERIALS AND METHODS

Materials

Humanized antibodies were provided by AbbVie-Stemcentrx (South San Francisco, CA). Site-specific antibodies of huIgG1, N149, and SC16.56 (also referred to as SC16) were genetically engineered with a C220S mutation. Pyrrolobenzodiazapene (PBD) dimer antibody-drug conjugates (ADCs) of N149 and SC16 were provided by AbbVie-Stemcentrx utilizing a cathepsin B cleavable PEG linker. All ADCs and RICs prepared and tested in this study are listed in Table 1, with corresponding properties such as their respective payload (PBD or radioisotope), whether they target the DLL3 protein, and whether conjugation is performed through site-specific (SS) or interchain disulfide reduction. ^{177}Lu trichloride was purchased through

Perkin-Elmer (Waltham, MA). ^{225}Ac trichloride was purchased from the National Isotope Development Center (Oak Ridge, TN), which is supported by the Isotope Program within the Office of Nuclear Physics in the Department of Energy's Office of Science. 1,4,7,10-Tetraazacyclododecane-1,4,7-tris-acetic acid-10-maleimidoethylacetamide (DOTA-MMA) was purchased from Macrocyclics (Plano, TX), Bradford reagent was purchased from Bio-rad (Hercules, CA), and tris(2-carboxyethyl)phosphine hydrochloride (TCEP HCl), L-glutathione reduced, and all other chemicals were purchased from Sigma-Aldrich (St. Louis, MO).

Table 1. List of ADCs and RICs studied in this work.

Nomenclature	Payload	Targeted Antibody	Conjugation Site-specificity
IgG1.ADC6.5	PBD	x	x
IgG1.ADC6.23 SS	PBD	x	√
SC16.15.ADC6.5	PBD	√	x
SC16.LD6.23D2 SS	PBD	√	√
SC16L6.5	PBD	√	x
SC16LD6.23	PBD	√	√
N149.ADC6.5	PBD	√	x
N149.ADC6.23 SS	PBD	√	√
^{177}Lu-IgG SS	^{177}Lu-DOTA-MMA	x	√
^{177}Lu-IgG	^{177}Lu-DOTA-MMA	x	x
^{225}Ac-IgG SS	^{225}Ac-DOTA-MMA	x	√
^{225}Ac-IgG	^{225}Ac-DOTA-MMA	x	x
^{177}Lu-SC16.56 SS	^{177}Lu-DOTA-MMA	√	√
^{177}Lu-SC16.56	^{177}Lu-DOTA-MMA	√	x
^{225}Ac-SC16.56 SS	^{225}Ac-DOTA-MMA	√	√
^{225}Ac-SC16.56	^{225}Ac-DOTA-MMA	√	x
^{177}Lu-N149 SS	^{177}Lu-DOTA-MMA	√	√
^{177}Lu-N149	^{177}Lu-DOTA-MMA	√	x
^{225}Ac-N149 SS	^{225}Ac-DOTA-MMA	√	√
^{225}Ac-N149	^{225}Ac-DOTA-MMA	√	x
DOTA-IgG SS	DOTA-MMA	x	√
DOTA-IgG	DOTA-MMA	x	x

Activity counting

All activity was measured via a Perkin-Elmer Tri-Carb 2910 TR with equilibrated sample in 10 mL of Ultima Gold LLT scintillation cocktail. In all experiments and figures, ^{225}Ac activity includes all daughter species in the decay chain at equilibrium. Biodistribution samples were counted on a Wallac 1470 Wizard gamma spectrometer.

Antibody reduction and conjugation with DOTA-MMA

Antibody conjugation was performed following two methods, depending on site-specific (*14*) or interchain disulfide reduction (native). Both antibody conjugation types started with batch reactions in the 20-400 µg mass region at a concentration range of 5-10 µg/mL. Native antibodies were first reduced with TCEP for 90 minutes in 0.2 M tris(hydroxymethyl)aminomethane (tris) + 0.05 mM ethylenediaminetetraacetic acid (EDTA) at pH 7.4 at room temperature under argon with a target drug-antibody ratio (DAR, where in the case of ^{225}Ac or ^{177}Lu conjugates, the 'drug' is the isotope-DOTA-MMA complex) of 4. To couple DOTA-MMA to site-specific antibodies, antibodies were first reduced in 1 M arginine with 7 mM glutathione at pH 8.0 for 2 hours at room temperature under argon with a target DAR of 2. Results of this are depicted in the Supporting Information. All buffer exchanges in the work were using 30 kDa Amicon spin filters. For both antibody types, antibody solutions were washed 10x volume four times and buffer exchanged into 0.2 M tris + 0.05 mM EDTA pH 7.4. A 50x excess DOTA-MMA to thiol sites was added, argon capped, and incubated at 2-5℃ overnight. 1.2:1 moles N-acetyl cysteine (NAC) to DOTA-MMA was added for 20 minutes at room temperature with argon. This solution was then buffer exchanged in ammonium acetate 0.2 M pH 5.4 to remove residual reactants and EDTA. After this stage, a DAR was found using

bench-top Arsenazo III metal competition assay for material reference, as described in the Supporting Information.

DOTA-MMA-Antibody radiolabeling

Caution: ^{177}Lu and ^{225}Ac are radioactive isotopes that may present serious health risks when internalized. Experiments were performed in facilities specially designed for the safe-handling of radioactive materials at the Lawrence Berkeley National Laboratory (LBNL).

A dry heating block was warmed to 45˚C and antibodies were pre-incubated for 5 minutes. The radionuclide in 0.05N HCl was added with 5x excess DOTA-MMA:^{177}Lu for 90 minutes, and with 200x excess DOTA-MMA:^{225}Ac for 2 hours. Both of these reactions proceeded at 45˚C. Metal excesses were based off of shipped specific activities, not accounting for daughters. Starting activity was based on an aliquot of the stock solution at equilibrium upon radiolabeling. After incubation, the antibody solutions were allowed to sit at room temperature for 10 minutes, and then 5-10x volume 10 mM EDTA was added to only the ^{225}Ac formulation for competition for 10 minutes. These radiolabeled solutions were washed and buffer exchanged (10x volume 5 times) into phosphate buffered saline (PBS) pH 7.4, and aliquots of filtrate and retentate were taken for final activity and yield verification.

Antibody-DOTA-MMA-radionuclide characterization

A Bradford assay (see Supporting Information) was performed to determine antibody protein concentration compared to internal huIgG1 standards, and liquid scintillation was used to count activity of the filtrate and retentate, using Perkin-Elmer Ultima Gold LLT liquid scintillation cocktail. These values were used to calculate the specific activity added in final formulations. For free metal

determination and serum stability, radio thin layer chromatography (TLC) was performed with a BioScan System 200 (10 mm, high efficiency collimator), using silica gel / glass TLC plates. The mobile phase consisted of de-ionized water pH shifted to 10.5 with KOH, with 50 mM EDTA to move free metal to Rf=1.

In vitro **cell killing studies**

In vitro cell killing studies were first performed on freshly prepared ADCs and radiolabeled RICs for an in-depth characterization of *in vitro* targeting and killing efficiency. However, in all subsequent *in vivo* studies, all formulations used for injections were also tested *in vitro*, to provide control data and verify that the determined IC50 values were unchanged in those formulations. Radiolabeled RICs were initially counted on LSC to determine activity, and protein concentration measured via Bradford assays (see Supporting Information). These solutions were then serial-diluted in 10 mM PBS pH 7.4 to desired activity concentrations. HEK-293T and HEK-293T-oxhSC16 (+DLL3 expressing, Hx16) human embryonic kidney epithelial cells were provided by AbbVie-Stemcentrx. Cells were grown in DMEM (Corning Cellgro, cat\#10-013-CV) supplemented with 10% fetal bovine serum (VWR Life Science Seradigm, cat\#1500-500), 1% penicillin-streptomycin (Corning Cellgro, cat\#30-002-CI) and 1% sodium bicarbonate (Corning Cellgro, cat\#25-035-CI). Cell cultures were maintained in a humidified atmosphere at 37˚C in 5% CO2/95% air. Cells were sub-cultured by removing the medium and incubating at room temperature with trypsin-versene (Corning Cellgro, cat\#25-053-CL) for 2-3 minutes or until cells detached. Cells were gently re-suspended in fresh medium and aliquoted into flasks (BD Falcon, cat\#353135). The initial seeded cell doubling rate was found to be roughly 18 hours. For cytotoxicity experiments, cells were seeded at 500 cells/well in 96-well plates (BD Falcon, cat\#353075) in 50 µL of culture

medium and incubated overnight in a 37˚C humidified incubator in 5% CO2. The following day the cell wells were given fresh media and treated with 40 µL of additional media combined with 10 µL of various antibody drug conjugates (ADCs, AbbVie-Stemcentrx) or RICs conjugated with ^{177}Lu or ^{225}Ac (serial dilutions were performed in 1x pH 7.4 PBS and then diluted in culture medium), for a total final volume of 100 µL. Each sample treatment consisted of 8 serial dilutions in 3 replicate wells. Following treatment addition, the 96-well plates were returned to the incubator for 4 days. Cytotoxicty was then measured using the CellTiter-Glo Luminescent Cell Viability Assay (Promega, cat\#3915) following the manufacturer's instructions. Briefly, 100 µL of the reagent was added to each well and the plate was incubated for 5 minutes at room temperature with mixing. For each well, 150 µL of the lysed cell solution was then transferred to black 96-well plates (Corning, cat\#3915) and the luminescence read using a SpectaFluor Plus Microplate Reader (Tecan). The luminescence for the sample wells was normalized to the no-treatment control wells for each plate. 4-parameter sigmoidal fit curves were used to determine IC50 values.

In vivo **mouse studies**

All procedures and protocols used in the described *in vivo* studies were reviewed and approved by the LBNL Institutional Animal Care and Use Committee (IACUC) and were performed in AAALAC accredited facilities. Antibodies were prepared with slight variation, where after final washing and buffer exchange into PBS prior to use, ascorbic acid was added to the solution to a resulting 5 mg/mL in the evening to hinder oxidative radiolysis (*15*), left overnight at 2-5˚C (before making this standard, the activity to reach 50% cell growth inhibition had been confirmed to be equal to using the material immediately, although specific activity is slightly reduced), and

washed the next day prior to use. Antibody preparations were then diluted with PBS pH 7.4 to appropriate concentrations and sterile filtered with 0.2 µm syringe filters into animal injection vials.

For the MTD study, 5-7 week-old female NOD SCID mice (Charles River Laboratories, NY, USA) were randomized to an average weight of 20.5 ± 1.4 g (n = 5 per group). Mice were injected intraperitoneally at 10 µL/g with 10 mg/kg pre-dose 30 minutes prior with huIgG1, followed by one of four dose response treatments, of either ^{177}Lu-IgG SS [32 to 860 MBq/kg (0.84 to 23.2 mCi/kg)] or ^{225}Ac-IgG SS [0.25 to 6.8 MBq/kg (6.8 to 180 µCi)/kg)]. Control animals were injected with non-radiolabeled DOTA-IgG SS. Mice were checked daily for signs of distress, and weights measured twice a week, for a 35-day endpoint.

For the PDX tumor efficacy study, 6-8-week-old female NOD SCID mice (Charles River Laboratories, NY, USA) were allowed to acclimatize for 1 week with food and water being provided *ad libitum* prior to PDX implantation. The Lu149 PDX line was used (moderate DLL3 expression, complete response to treatment with SC16.56 followed by relapse). The PDX tumors were passaged in mice and prepared as single cell suspensions (1.5 - 3 million cells) in 1:1 PBS/Matrigel prior to subcutaneous transplantation in the right mammary fat pad of NOD SCID mice under isoflurane anesthesia. Mice were randomized for efficacy studies 5 – 9 weeks after the subcutaneous transplantation, when the tumors reached a volume of 142.7 ± 51.6 mm^3, with a corresponding body weight of 26.7 ± 2.2 g. Tumor-bearing mice (n = 5 per group) were injected intraperitoneally at 10 µL/g with 10 mg/kg pre-dose 30 minutes prior with huIgG1, followed by the appropriate immunoconjugate treatment: huIgG1, N149, or SC16.56 site-specific conjugated with PBD [1.6 mg/kg], ^{177}Lu-DOTA-MMA [0.8 mg/kg; 670 µCi/kg], or ^{225}Ac-DOTA-MMA

[0.02 mg/kg; 8 µCi/kg]. Mice were checked daily for signs of distress, and weights and tumor volumes measured twice a week. Mice were euthanized by cervical dislocation if tumor volumes were larger than 1,000 mm^3 for two consecutive measurements.

Intraperitoneal injection was chosen over intravenous due to two factors, 1) high consistency of successful injections, 2) rapidity of injections when working with large animal sets, 3) minor differences in biodistribution after the first hour of intraperitoneal vs intravenous injection.

For the biodistribution study with ^{125}I and ^{225}Ac, mice were prepared similarly to the PDX efficacy study above. Tumor-bearing mice (n = 3 per group) were injected intraperitoneally at 10 µL/g with 10 mg/kg pre-dose 30 minutes prior with huIgG1, followed by the appropriate immunoconjugate treatment: huIgG1 or SC16.56 site-specific conjugated with PBD [1.6 mg/kg] + I-125 [4 µCi/kg], or ^{225}Ac-DOTA-MMA [0.02 mg/kg; 8 µCi/kg]. Iodine Radiolabeling was performed with $Na^{125}I$ (Perkin Elmer, Boston, MA) using the Iodogen method (Pierce, Rockford, IL). Unbound iodine was removed via 30kDa Amicon spin filters. Mice were checked daily for signs of distress, and weights and tumor volumes measured twice a week. Mice were euthanized by cervical dislocation if tumor volumes were larger than 1,000 mm^3 for two consecutive measurements. Time points were taken and samples were gamma counted on a Wallac 1470 Wizard gamma spectrometer, accounting for counting delay and isotope efficiency. The two windows of gamma emission tracked were 1-40 keV for I-125 (35 keV), and 180-490 keV for ^{225}Ac daughters Fr-221 (218 keV) and Bi-213 (440 keV).

RESULTS

Antibody conjugation and radiolabeling

For native-state interchain disulfide antibodies, a drug-antibody ratio (DAR) target of 4 DOTA-MMA per antibody was chosen for reduction, and site-specific antibodies were targeted for a DAR of 2 due to engineered cysteine sites on the light chains. PBD-dimer conjugates constructed at AbbVie-Stemcentrx contained a DAR of 2 PBD:mAb. Upon optimization of the reduction step, these DAR target values were verified to reach approximately the correct number of reduced cysteine sites via a combination of Ellman's free thiol assay and Bradford protein assays (**Figure S1 A, B**). After reduction, DOTA-MMA was conjugated to the free thiol sites, and optimized via a combination of an Arsenazo (III) assay with Eu^{3+} and a Bradford assay to estimate the number of DOTA-MMA sites present per antibody.

With these DOTA-MMA-conjugated antibodies, we then proceeded with radiolabeling. We found that 45℃ for 2 hours with ^{225}Ac, and 45℃ for 90 minutes with ^{177}Lu showed optimal DOTA-MMA-metal binding, similar to the conditions found in McDevitt et al. (*16*) to minimize denaturation. With the excess of DOTA-MMA:metal in the radiolabeling step (molar ratios of 5:1 ^{177}Lu, 200:1 ^{225}Ac), the resulting metal to antibody ratio is therefore significantly less than the DAR values found for small molecule drugs (see **Figure S1 E**). The resulting specific activities prior to dilution are shown in **Figure S1 F**.

After radiolabeling with the ^{225}Ac/daughter mixture and washing the predominantly ^{225}Ac-DOTA-MMA-mAb complex, the total time to liquid scintillation counting (LSC) is approximately 0.05 days (1.2 hours) for dose preparations. Modeled in **Figure 2** is the fractional power of each species at time(t) divided by ^{225}Ac (A) or ^{177}Lu (B) at

time(0), where time(0) is the time of LSC analysis. However, since ^{225}Ac daughters generate rapidly after washing, time(0) starts at species equilibrium concentrations time(0.05) days (1.2 hours) after purification, where there is already over 400% of the initial ^{225}Ac power (and activity) in sum. Since ^{177}Lu has no radioactive daughters, there is no increase in power or activity over time after purification.

Radio-TLC analysis was performed for each sample in each experiment to ensure high bound-activity of the constructs. For ^{225}Ac RICs, while solutions were developed immediately after preparation, a waiting period of 24 hours was required to remove any initial unbound daughters from the Rf=1 free metal position. This TLC paradigm is modeled in **Figure S1 D**. In the mobile phase, which contained 50 mM EDTA, EDTA transported free metal to Rf = 1, while antibody-DOTA-MMA and antibody-DOTA-MMA-metal remains at Rf = 0, and any free DOTA-MMA was found to travel near Rf = 0.5. Compared to DOTA-MMA-radionuclide controls, we did not see unbound DOTA-MMA-radionuclide peaks in our sample preparations, indicating good antibody-DOTA-MMA conjugate stability. Serum stability of ^{225}Ac RICs showed 100% association with the DOTA-MMA-mAb complex up to 6 days after treating with an EDTA challenge, post-conjugation, whereas ^{177}Lu RICs remained stable throughout the assay (see **Figure S1 C**). We note that radio-TLC analysis does not allow to unequivocally distinguish radioisotopes bound to intact antibodies or to large degraded protein fragments. Therefore, the possibility exists that a fraction of the antibody proteins within the RICs (even when deemed stable by radio-TLC) may have lost some integrity.

In vitro **cell killing**

Using 293T cells with and without DLL3 expression (*5*) (293T-Hx16 is +DLL3, 293T is -DLL3), cell viability curves were established over 4 day incubation with ^{225}Ac and ^{177}Lu DOTA-MMA-mAb. Comparing non-targeted DOTA-MMA-huIgG1 conjugates to targeted humanized antibody SC16.56, the antibody half-maximal inhibitory concentration (IC50) values were found to be dependent only on radioactivity, and independent on antibody concentration, as can be seen by the differing specific activity values between native and site-specific antibodies of **Figure S1 F**, but highly similar activity cell killing profiles and IC50 values of **Figure 3**. ^{225}Ac site-specific SC16.56 conjugates only required 5.37 ± 1.22 Bq/100 µL (145 ± 33 pCi/100 µL) activity to reach the IC50, compared to 13.7 ± 2.8 kBq/100 µL (370 ± 76 nCi/100 µL) activity per volume for ^{177}Lu SC16.56 constructs. On average for non-targeted DOTA-MMA-huIgG1 on either cell line, and targeted constructs on -DLL3 cells, there was a 214 ± 49 times increased activity required for ^{177}Lu vs ^{225}Ac, with no drastic changes between native and site-specific antibody conjugation methods (**Figure 3**). However, for targeted constructs on +DLL3 HEK-293T cells, ^{177}Lu required 1278 ± 384 times more activity compared to ^{225}Ac. Another antibody that recognizes the often over-expressed antigen CD46 (*17*), N149, was used as a positive control and showed less *in vitro* activity on 293T +DLL3 expressing cells, at a range similar to non-specific controls (see **Figure S2 E, F**). PBD-dimer containing ADCs were also tested, finding a range from low pM to nM IC50s (see **Figure S2 A, B, C, D**). Due to the well-described benefits of site-specific conjugation (*18*), and similar IC50 values found, subsequent experiments in this work are focused only on the site-specific constructs. IgG1.ADC6.23 site-specific (SS), N149.ADC6.23 SS, and SC16.LD6.23D2 SS were used in the remaining studies as control PBD-dimer ADCs.

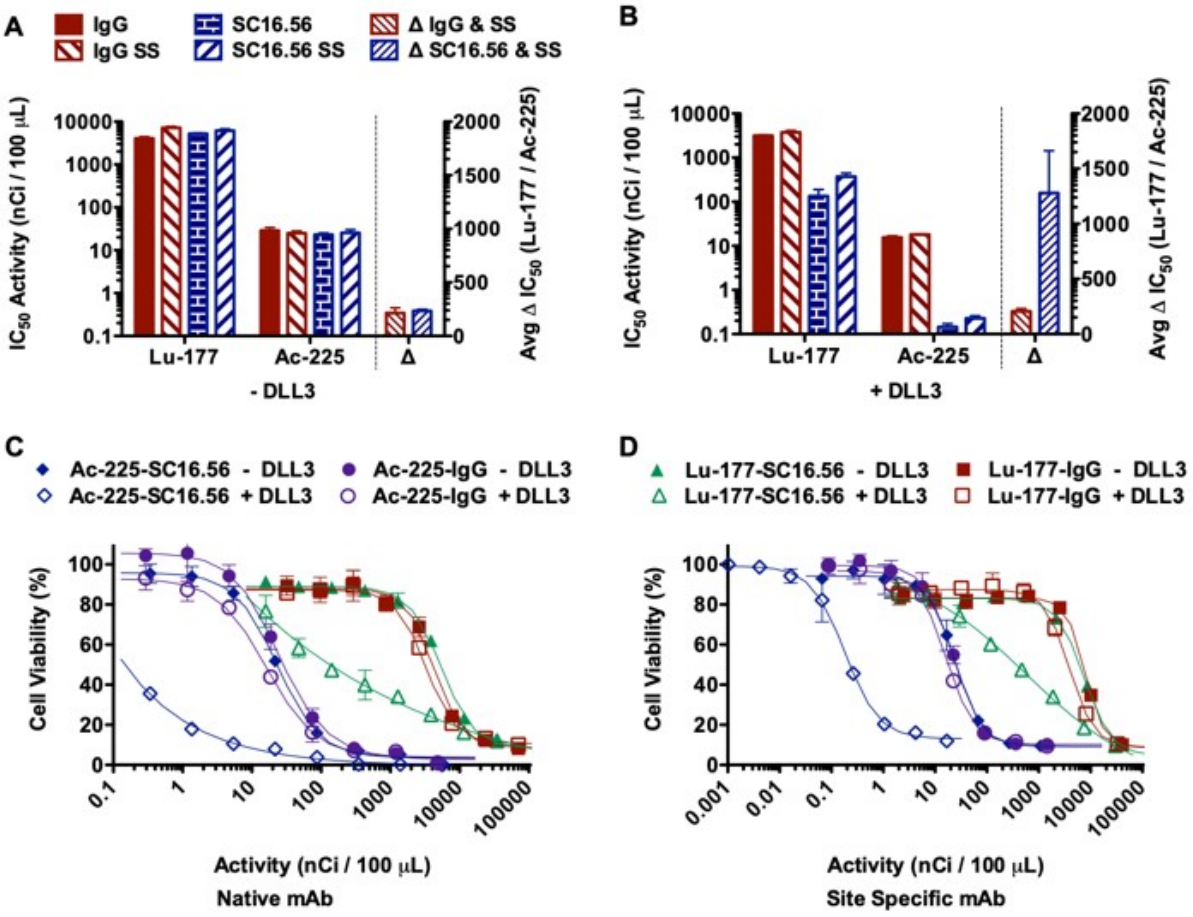

Figure 3. *In vitro* cell toxicity comparison of radionuclide-DOTA-MMA-mAb conjugates. Top: IC50 values for 293T (**A**, -DLL3) and 293T-Hx16 (**B**, +DLL3) cells exposed to ^{225}Ac or ^{177}Lu DOTA-MMA RICs of non-targeting huIgG1 or targeting SC16.56; 'ΔAvg' is an average of both native and site-specific (SS) IC50 values of ^{177}Lu divided by ^{225}Ac. Δ bars correspond to the right y-axis showing differential IC50 values. Bottom: IC50 curves for natively conjugated (**C**) and site-specifically conjugated (**D**) ^{225}Ac or ^{177}Lu DOTA-MMA RICs. n=6, mean ± stdev.

NOD SCID mouse maximum tolerated dose

To determine maximum tolerated dose (MTD) for efficacy studies, non-targeted site-specific radioisotope-DOTA-MMA-huIgG1 conjugates were produced and radiolabeled with either ^{225}Ac or ^{177}Lu to test 4 different activities. NOD SCID mice were used for establishing PDX and were the adequate model for subsequent efficacy studies. Group survival and weight loss (represented as weight fraction relative to weight at time of injection) are shown in **Figure 4**. Animal groups that met the minimum health criteria at 5 weeks after injection were considered as tolerant to the dose given. For ^{225}Ac, the MTD was found to be 18.9-55.5 kBq (0.51-1.5 µCi) per 25 g mouse, or 0.74-2.22 kBq/g (20-60 nCi/g). In contrast, the MTD for ^{177}Lu was found to be between 0.77-2.37 MBq (21-64 µCi) per 25 g mouse, or 31.1-94.7 kBq/g (0.84-2.56 µCi/g). These ranges were taken into account for subsequent efficacy studies.

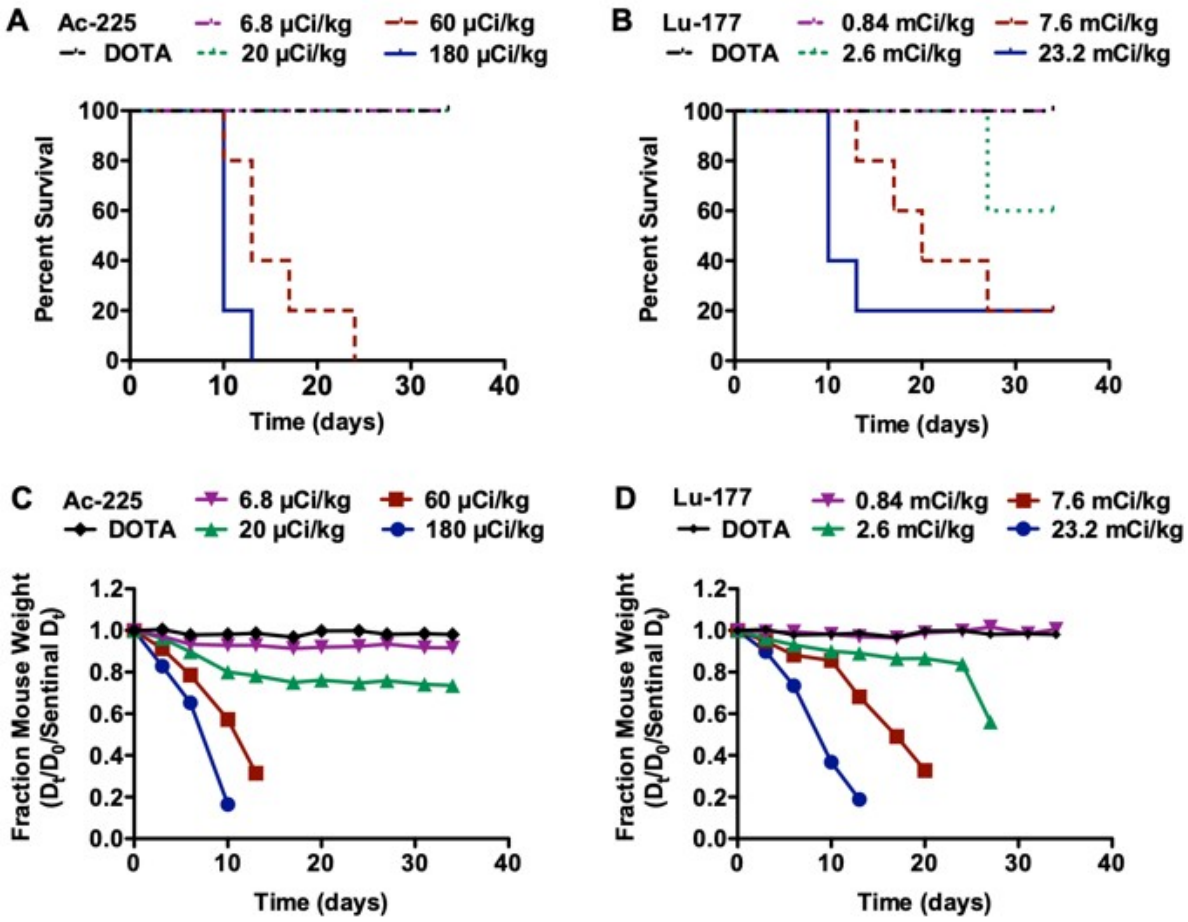

Figure 4. Maximum tolerated dose (MTD) determination for radionuclide-DOTA-MMA-mAb SS conjugates. RICs given to groups of healthy NOD SCID mice (n=5, mean ± stdev) by intraperitoneal injection. Top: Percent survival curves for animals injected with ^{225}Ac (**A**, 0.25 to 6.66 MBq/kg or 6.8 to 180 µCi/kg) or ^{177}Lu (**B**, 31.1 to 858 MBq/kg or 0.84 to 23.2 mCi/kg) RICs; control animals (labeled DOTA) were given the non-radiolabeled DOTA-MMA-mAb SS conjugate. Bottom: Corresponding average weight loss for ^{225}Ac (**C**) and ^{177}Lu (**D**) RICs.

PDX solid tumor efficacy and Biodistribution

For generation and propagation of PDX tumors, refer to Anderson et al. 2015 (*19*). When PDX solid tumors reached approximately 100 mm^3, animals were injected intraperitoneally with a pre-dose of unloaded site-specific huIgG1 30 minutes prior to injection with 1) site-specific DOTA-MMA-huIgG1 (negative control), 2) site-specific DOTA-MMA-N149, or 3) site-specific DOTA-MMA-SC16 antibodies, which were either radiolabeled with ^{225}Ac or ^{177}Lu, or were bound with PBD conjugate as positive controls. After 77 days of monitoring, group survival is shown in **Figure 5**. Cohorts that showed the greatest survival were the PBD controls, for which there was complete survival of the SC16.56-PBD group, and only one loss in the N149-PBD group. huIgG1-PBD was ineffective. For the ^{225}Ac RIC groups, N149 and SC16 showed similar efficacy, with 50% life expectancy-to-euthanasia extended from the 36 days huIgG1 control, to 64 days for both N149 and SC16. For ^{177}Lu RIC groups, the huIgG1 control showed 50% life expectancy-to-euthanasia at 37 days, and the N149 and SC16 extended 50% life expectancy out to 44 days and 45 days respectively (see **Figure S4**). Tumor growth rates can be seen in **Figure 6**, where targeted N149 and SC16-PBD groups showed near complete tumor volume recession over 50 days with 9/10 mice. ^{225}Ac mice showed tumor control over roughly 25 days before regrowth occurred, compared to the controls where growth was consistent throughout the time period. ^{177}Lu mice also showed some growth control, but perhaps not as dramatic as the ^{225}Ac groups. Interestingly, compared to the non-radiolabeled/non-PBD DOTA-MMA-huIgG1 control (**Figure S5)**, all other non-targeted huIgG1 control groups showed slower tumor growth. In addition, the growth trends for the radiolabeled antibodies are slower than that of the PBD control.

In complement to the tumor growth control studies, a biodistribution study was performed on a similar set of tumor-bearing mice (see **Figure S6**). ^{125}I was tyrosine-labeled on huIgG1-PBD and huSC16-PBD. Using two detection windows on a gamma counter (^{125}I, ^{221}Fr + ^{213}Bi), we tracked biodistribution over 20 days for both ^{125}I and ^{225}Ac after pre-injection with 10 mg/kg unlabeled huIgG1. ^{225}Ac tumor uptake at 20 days was 4.5 ± 0.6 %RD/g for IgG and 5.9 ± 0.3 %RD/g for SC16. PBD constructs showed similar %RD/g values for SC16-PBD (4.5 ± 0.4 %RD/g), but much lower compared to huIgG1-PBD (0.6 ± 0.03 %RD/g).

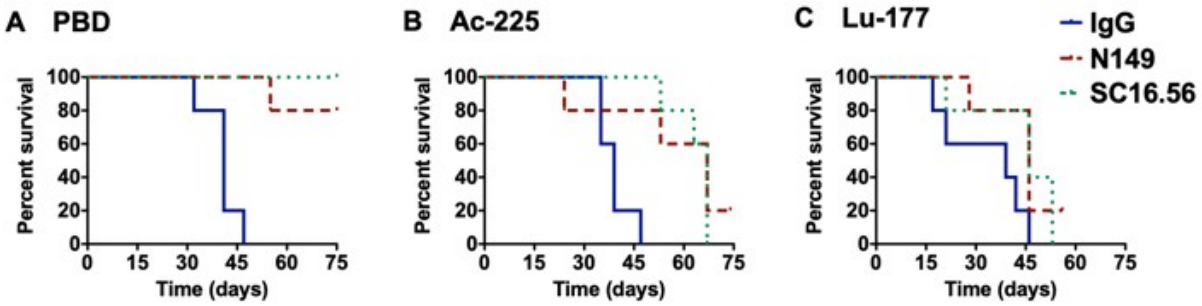

Figure 5. Survival of PDX NOD SCID mice (n=5, mean ± stdev) injected intraperitoneally with the appropriate site-specific immunoconjugate treatment: huIgG1, N149, or SC16.56 conjugated with PBD (**A**, 1.6 mg/kg), ^{225}Ac-DOTA-MMA (**B**, 0.02 mg/kg; 296 kBq/kg or 8 µCi/kg), or ^{177}Lu-DOTA-MMA (**C**, 0.8 mg/kg; 24.8 MBq/kg or 670 µCi/kg).

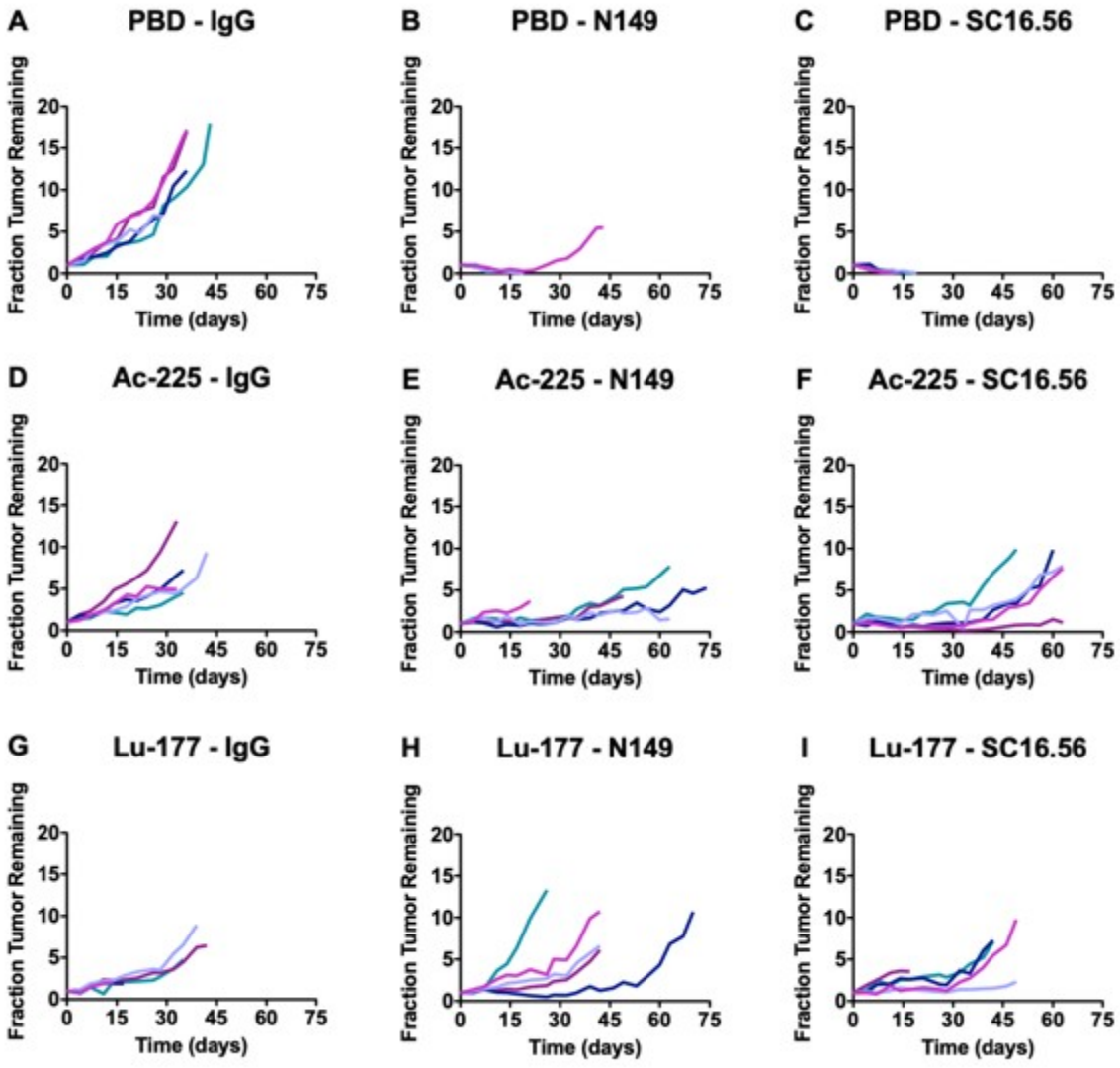

Figure 6. Fraction of remaining tumor volume from initial time point in PDX NOD SCID mice injected intraperitoneally with the appropriate immunoconjugate treatment: PBD (**A**, **B**, and **C**; 1.6 mg/kg), ^{225}Ac-DOTA-MMA (**D**, **E,** and **F**; 0.02 mg/kg; 296 kBq/kg or 8 µCi/kg), or ^{177}Lu-DOTA-MMA (**G**, **H**, and **I**; 0.8 mg/kg; 24.8 MBq/kg or 670 µCi/kg) conjugated with huIgG1, N149, or SC16.56. Each line represents one animal.

DISCUSSION

Targeted alpha therapy (TAT) RICs are an exciting addition to small-molecule drug chemotherapeutics and antibody drug conjugates. In particular, ^{225}Ac, with a 10-day half-life and 3 rapid-fire α emissions (^{225}Ac, Fr-221, At-217), presents a potent delivery package on the order of mAb circulatory half-lives. Considering the multitude of variables driving efficacy in antibody therapies, such as circulatory half-life, dose, immunogenicity, target binding/uptake, linker release, etc., RICs have the additional variable of radioactive half-life. This component may increase the therapeutic window at the target site, mimicking that of extended release pharmaceutical formulations, and dampen the rate of non-specific toxicity. In the case of the only FDA approved RIC, the diethylenetriamine pentaacetic acid- (DTPA-) based ^{111}In/^{90}Y Ibritumomab tiuxetan (Zevalin), the extended dosimetry requires only a single patient infusion (*20*). The four approved ADCs (*14*) typically require multiple patient-infusion visits to receive multiple doses for highest efficacy (*21*,*22*), offering a potential savings to the patient in not only minimizing patient visits and compliance, but monetarily as well.

Nonetheless, even with increasing interest in targeted alpha therapies using ^{225}Ac (*16*,*23*,*32–34*,*24–31*), there is still only one published work comparing ^{225}Ac vs ^{177}Lu RICs for solid tumors, a prostate cancer RIC of huM195-DOTA-MMA-^{225}Ac on nude mice (*16*), and none that compare to small molecule loaded antibody-drug conjugates to the best of the authors knowledge. Further, the Scheinberg et al. (*35*) comparison of ^{225}Ac and ^{177}Lu showed a similar MTD value in naive nude mice (18.5 kBq or 500 nCi) with untargeted IgG-DOTA-MMA-^{225}Ac to what we found with NOD SCID mice (18.9 kBq or 510 nCi) with untargeted IgG-DOTA-MMA-^{225}Ac. Considering NOD SCID mice are more highly immunosuppressed to nude mice, it again signals

the acute non-specific toxicity is independent of the immune system. *In vitro* cell killing in later published data (*35*) showed IC50 activity from 296 mBq/mL (8 pCi/mL) using huM195-DOTA-MMA-^{225}Ac on HL60 cells, to 48.1 Bq/mL (1300 pCi/mL) using Herceptin-DOTA-MMA-^{225}Ac on SKOV3-NMP2 cells. These results are on the same order as what was observed in this work, which showed a lowest IC50 activity of 53.7 ± 12.2 Bq/μL (1450 ± 330 pCi/μL) using our huSC16-DOTA-MMA-^{225}Ac antibody on +DLL3 HEK-293T-Hx16 cells. Given the broad range of cytotoxicity *in vitro*, and our construct being on the lower end of cytotoxicity compared to previous work (*16*), it is apparent that this SCLC model may be difficult to treat in comparison to other cancers (*36*). McDevitt et al. also compared *in vitro* serum stability at 37 ºC of huM195-DOTA-MMA with either ^{225}Ac or ^{177}Lu, and found similar stability to our work, with up to 5% dissociation of the ^{225}Ac construct (*16*).

Conjugation of ^{225}Ac resulted in relatively low yields for ^{225}Ac, typically on the order of 1-5 % after EDTA challenge. This was while using a 200:1 DOTA-MMA:Metal molar ratio, and thus the resulting number of metals per antibody was roughly 1 in 100 (DAR) after final formulation for use, whereas ^{177}Lu was often nearly quantitative, and produced roughly 1 in 10 (DAR) antibodies being radiolabeled. In contrast to the DAR = 2 for the PBD ADCs, these values are much lower. While the DAR of approved small molecule ADCs are averages of 4 for Brentuximab vedotin (*37*), 3.5 for Trastuzumab emtansine (*38*), 4 for Gemtuzumab ozogamicin (*39*), and 6 for Inotuzumab ozogamicin (*40*), creating a deliverable RIC with a radioisotope DAR in the 2-6 may not be feasible for delivery. Such high radioisotope content would not only require a minuscule amount of antibody to be delivered, but it would likely lessen the radioisotope yield, increase the amount of unbound activity, and may increase radiolysis. Comparing these formulations to Zevalin (targets CD20 (*41*,*42*)),

as can be determined from the FDA accepted package insert documents (*43*), there is a final formulation maximum specific activity of approximately 62.9kBq and 462.5 kBq/µg (1.7 and 12.5 µCi/µg) for ^{111}In and ^{90}Y respectively, resulting in an approximate maximum (DAR equivalent) of 1 in 200 (0.005) and 1 in 25 (0.04) metals per antibody for ^{111}In and ^{90}Y respectively. These specific activities and metal/antibody ratios correspond very similarly to those produced in this work (see **Figure S1 E, F**). Additional radiolabeling considerations are provided in the Supporting Information.

In vitro studies produced effective sub-nCi IC50 activities on +DLL3 cells using targeted ^{225}Ac RICs, and sub-µCi for targeted ^{177}Lu RICs. However, the targeting ratio of ^{225}Ac vs ^{177}Lu RICs was dramatically different for targeted vs non-specific RICs, with ^{225}Ac showing much greater cell killing at over 1200 times greater ^{177}Lu activity required vs ^{225}Ac (see **Figure 3**). Comparing to Graf et al. (*13*), ^{177}Lu-DOTATOC required 700 times more activity than ^{225}Ac-DOTATOC on somatostatin expressing neuroendocrine AR42J cells *in vitro*. For *in vivo* studies with in BALB/c nu/nu mice, the same 700 times increased ^{177}Lu activity over ^{225}Ac inhibited tumor growth for 15 days (*13*).

Similarly to the non-specific huIgG RICs ratio of IC50 *in vitro*, the MTD study showed dose tolerance just over 120 times more ^{177}Lu / ^{225}Ac (see **Figure 4** and **Figure S3**). Even though in the tumor efficacy study, ^{225}Ac and ^{177}Lu RICs were dosed at the MTD, ^{225}Ac RICs performed better than ^{177}Lu with both targeted antibodies, with extended life expectancy and tumor growth suppression. For both radioisotopes, the targeted RICs performed better than the non-specific huIgG1 RICs (see **Figure S4 A, B**). However, the small molecule PBD-dimers were very effective for this

particular SCLC PDX model, and performed impressively with 9/10 mice showing complete tumor control.

In the biodistribution study (see **Figure S6**), ^{225}Ac %RD/g was greater than ^{125}I %RD/g across all tissues in huIgG and SC16. A large dissimilarity is also observed between the time-dependent biodistribution profiles of the targeted constructs of SC16-DOTA-MMA-^{225}Ac and SC16-PBD dimer, especially in the spleen and liver. In the case of the SC16-PBD dimer, spleen and liver burdens decrease over time, perhaps due to dehalogenization *in vivo*, but also potentially indicative of antibody clearance from these off-target organs. In contrast, ^{225}Ac content, especially in the liver, remains high even at 20 days post-injection. It is therefore likely that ^{225}Ac is dissociating from the antibody construct over time and being redistributed to or retained within these off-target organs. While tumor uptake was low across the board compared to spleen and liver, the targeted constructs of SC16-DOTA-MMA-^{225}Ac and SC16-PBD dimer were greater at 20 days than the untargeted controls. The difference in tumor uptake for targeted vs untargeted was greater for PBD, further supporting the greater efficacy of tumor suppression in PBD constructs. Non-radiolabeled untargeted huIgG1 antibody was again pre-dosed at 10 mg/kg for both efficacy and biodistribution studies. Due to the small mass of total antibody injected compared to the total typical circulating concentration (from 1-5 mg/mL huIgG1), pre-dosing was estimated to not saturate the pinocytotic FcRn antibody recycling process, but minimize detrimental opsonization of the target formulation, thereby decreasing non-specific uptake, extending the circulation half-life, and increasing tumor dose (*44*). However, it is possible that with the extremely small mass of radiolabeled therapeutic antibody injected, immune system opsonization still managed to sequester activity away from the tumor sites compared to the high

mass dose of PBD ADC. Further, destructive recoil of ^{225}Ac and/or daughters *in vivo* over a 20-day period may have led to the higher untargeted tumor ^{225}Ac signal, and may be ultimately limiting the MTD which led to outperformance by the PBD ADC. Overall, these results reflect an inherent toxicity issue associated with the proposed used of antibodies radiolabeled with high linear energy transfer isotopes such as ^{225}Ac for therapeutic applications: despite efficient tumor targeting, the *in vivo* residence time of these large biogenics is usually significantly longer than that of smaller common targeting peptides, which results in a higher likelihood of undesired release and deposition of the radioisotope in non-targeted tissues.

CONCLUSIONS

New treatment options for cancer patients are under rapid development. In particular, targeted alpha therapies represent a future market with unique properties other anti-cancer therapies cannot offer. However, in this work and system, using matched antibodies with PBD dimers, ^{225}Ac, and ^{177}Lu constructs, it is apparent in this SCLC solid tumor system that PBD dimers showed superior tumor efficacy. This work has identified challenges in targeted radiotherapy development with the targeting agent, and while much development is still required in matching the application of α emitters to particular tumor types, there undoubtedly remains strong excitement in the massive potency α emitters may provide, with particular focus on sufficient construct targeting and stability.

ASSOCIATED CONTENT

Supporting Information

Extended experimental methods on conjugated and radiolabeled antibodies (Ellman, Bradford, and Arsenazo III assays); additional discussion on specific activity determination in radiolabeled immunoconjugates to take into account daughter nuclide generation; additional results including drug/antibody ratio determination, cell viability data, MTD comparisons, PDX tumor efficacy comparisons, and radiolabel biodistribution data.

CONFLICT OF INTEREST

The authors declare no competing financial interest.

AUTHOR INFORMATION

Corresponding Author. *E-mail: abergel@berkeley.edu.

ORCID

Dahlia D. An: 0000-0002-8763-6735

Julian A. Rees: 0000-0003-0883-2680

Rebecca J. Abergel: 0000-0002-3906-8761

ACKNOWLEDGEMENTS

This work was supported by AbbVie-Stemcentrx, LLC and performed at LBNL, operating under U.S. Department of Energy Contract (DOE) No. DE-AC02-05CH11231 (R.J.A.).

REFERENCES

1. Wang S, Tang J, Sun T, et al. Survival changes in patients with small cell lung cancer and disparities between different sexes, socioeconomic statuses and ages. *Sci Rep*. 2017;7:1-13.

2. Dayen C, Debieuvre D, Molinier O, et al. New insights into stage and prognosis in small cell lung cancer: An analysis of 968 cases. *J Thorac Dis*. 2017;9:5101.

3. Rudin CM, Pietanza MC, Bauer TM, et al. Rovalpituzumab tesirine , a DLL3-targeted antibody-drug conjugate , in recurrent small-cell lung cancer : a fi rst-in-human , fi rst-in-class , open-label , phase 1 study. *Lancet Oncol*. 2017;18:42-51.

4. Carlin SD, Sisodiya V, Hamdy O, et al. Noninvasive Interrogation of DLL3 Expression in Metastatic Small Cell Lung Cancer. *Cancer Res*. 2017;77:3931-3941.

5. Saunders LR, Bankovich AJ, Anderson WC, et al. A DLL3-targeted antibody-drug conjugate eradicates high-grade pulmonary neuroendocrine tumor-initiating cells in vivo HHS Public Access. *Sci Transl Med*. 2015;7:302-136.

6. Antczak C, Jaggi JS, Lefave C V, Curcio MJ, Michael R, Scheinberg D a. Influence of the Linker on the Biodistribution and Catabolism of Actinium-225 Self-Immolative Tumor-Targeted Isotope Generators. *Bioconjug Chem*. 2008;17:1551-1560.

7. Birrer MJ, Moore KN, Betella I, Bates RC. Antibody-Drug Conjugate-Based Therapeutics: State of the Science. *J Natl Cancer Inst*. 2019;111:538-549.

8. Maguire WF, McDevitt MR, Smith-Jones PM, Scheinberg DA. Efficient 1-step radiolabeling of monoclonal antibodies to high specific activity with ^{225}Ac for α-particle radioimmunotherapy of cancer. *J Nucl Med*. 2014;55:1492-1498.

9. McDevitt MR, Ma D, Simon J, Frank RK, Scheinberg DA. Design and synthesis of 225Ac radioimmunopharmaceuticals. *Appl Radiat Isot*. 2002;57:841-847.

10. Kozempel J, Mokhodoeva O, Vlk M. Progress in targeted alpha-particle therapy. What we learned about recoils release from in vivo generators. *Molecules*. 2018;23.

11. Seidl C. Radioimmunotherapy with α-particle-emitting radionuclides. *Immunotherapy*. 2014;6:431-458.

12. Emmett L, Willowson K, Violet J, Shin J, Blanksby A, Lee J. Lutetium 177 PSMA radionuclide therapy for men with prostate cancer: a review of the current literature and discussion of practical aspects of therapy. *J Med Radiat Sci*. 2017;64:52-60.

13. Graf F, Fahrer J, Maus S, et al. DNA double strand breaks as predictor of efficacy of the alpha-particle emitter 225Ac and the electron emitter ^{177Lu} for somatostatin receptor targeted radiotherapy. *PLoS One*. 2014;9.

14. Forte N, Chudasama V, Baker JR. Homogeneous antibody-drug conjugates via site-selective disulfide bridging. *Drug Discov Today Technol*. 2018;30:11-20.

15. Chakrabarti MC, Le N, Paik CH, De Graff WG, Carrasquillo J a. Prevention of radiolysis of monoclonal antibody during labeling. *J Nucl Med*. 1996;37:1384-1388.

16. McDevitt MR, Ma D, Lai L, et al. Tumor Therapy with Targeted Atomic

Nanogenerators. *Science (80-)*. 2001;294:1537-1540.

17. Fishelson Z, Donin N, Zell S, Schultz S, Kirschfink M. Obstacles to cancer immunotherapy: Expression of membrane complement regulatory proteins (mCRPs) in tumors. Mol. Immunol. 2003;40:109-123.

18. Behrens CR, Liu B. Methods for site-specific drug conjugation to antibodies. *MAbs*. 2014;6:46-53.

19. Anderson WC, Boyd MB, Aguilar J, et al. Initiation and characterization of small cell lung cancer patient-derived xenografts from ultrasound-guided transbronchial needle aspirates. *PLoS One*. 2015;10: e0125255.

20. Green DJ, Press OW. Whither Radioimmunotherapy: To Be or Not To Be? *Cancer Res*. 2017;77:2191-2196.

21. Chen Q, Ayer T, Nastoupil LJ, Rose AC, Flowers CR. Comparing the cost-effectiveness of rituximab maintenance and radioimmunotherapy consolidation versus observation following first-line therapy in patients with follicular lymphoma. *Value Heal*. 2015;18:189-197.

22. Al-Salama ZT. Inotuzumab Ozogamicin: A Review in Relapsed/Refractory B-Cell Acute Lymphoblastic Leukaemia. *Target Oncol*. 2018;13:525-532.

23. Behling K, Maguire WF, Di Gialleonardo V, et al. Remodeling the Vascular Microenvironment of Glioblastoma with -Particles. *J Nucl Med*. 2016;57:1771-1777.

24. Escorcia FE, Henke E, Mcdevitt MR, et al. Selective Killing of Tumor Neovasculature Paradoxically Improves Chemotherapy Delivery to Tumors. 2010:9277-9287.

25. Miederer M, McDevitt MR, Sgouros G, Kramer K, Cheung N-K V, Scheinberg DA. Pharmacokinetics, dosimetry, and toxicity of the targetable atomic generator, 225Ac-HuM195, in nonhuman primates. *J Nucl Med*. 2004;45:129-37.

26. Nedrow JR, Josefsson A, Park S, et al. Pharmacokinetics, microscale distribution, and dosimetry of alpha-emitter-labeled anti-PD-L1 antibodies in an immune competent transgenic breast cancer model. *EJNMMI Res*. 2017;7:57.

27. Behling K, Maguire WF, Carlos L, et al. Vascular Targeted Radioimmunotherapy for the Treatment of Glioblastoma. 2016;57:1576-1582.

28. Jaggi JS, Kappel BJ, McDevitt MR, et al. Efforts to control the errant products of a targeted in vivo generator. *Cancer Res*. 2005;65:4888-4895.

29. Miederer M, McDevitt MR, Borchardt P, et al. Treatment of neuroblastoma meningeal carcinomatosis with intrathecal application of α-emitting atomic nanogenerators targeting disialo-ganglioside GD2. *Clin Cancer Res*. 2004;10:6985-6992.

30. Lengana T, Mahapane J, Lawal I, et al. 225Ac-PSMA-617 in chemotherapy-naive patients with advanced prostate cancer: a pilot study. *Eur J Nucl Med Mol Imaging*. 2018;46:129-138.

31. Kennel SJ, Chappell LL, Dadachova K, et al. Evaluation of 225 Ac for Vascular Targeted Radioimmunotherapy of Lung Tumors. *Cancer Biother Radiopharm*. 2002;15:235-244.

32. Yoshida T, Jin K, Song H, et al. Effective treatment of ductal carcinoma in situ with a HER-2- targeted alpha-particle emitting radionuclide in a preclinical

model of human breast cancer. *Oncotarget*. 2016;7:33306.

33. Kratochwil C, Schmidt K, Afshar-Oromieh A, et al. Targeted alpha therapy of mCRPC: Dosimetry estimate of 213Bismuth-PSMA-617. *Eur J Nucl Med Mol Imaging*. 2018;45:31-37.

34. Borchardt PE, Yuan RR, Miederer M, McDevitt MR, Scheinberg DA. Targeted actinium-225 in vivo generators for therapy of ovarian cancer. *Cancer Res*. 2003;63:5084-5090.

35. A. Scheinberg D, R. McDevitt M. Actinium-225 in Targeted Alpha-Particle Therapeutic Applications. *Curr Radiopharm*. 2011;4:306-320.

36. Chakravarty R, Siamof CM, Dash A, Cai W. Targeted α-therapy of prostate cancer using radiolabeled PSMA inhibitors: a game changer in nuclear medicine. *Am J Nucl Med Mol Imaging*. 2018;8:247.

37. Chen L, Wang L, Shion H, et al. In-depth structural characterization of Kadcyla® (ado-trastuzumab emtansine) and its biosimilar candidate. *MAbs*. 2016;8:1210-1223.

38. Hurvitz SA, Dirix L, Kocsis J, et al. Phase II randomized study of trastuzumab emtansine versus trastuzumab plus docetaxel in patients with human epidermal growth factor receptor 2-positive metastatic breast cancer. *J Clin Oncol*. 2013;31:1157-1163.

39. Zaro JL. Mylotarg: Revisiting Its Clinical Potential Post-Withdrawal. In: Wang J, Shen W-C, Zaro JL, eds. Antibody-Drug Conjugates: The 21st Century Magic Bullets for Cancer. Cham: Springer International Publishing; 2015:179-190.

40. Bouchard H, Viskov C, Garcia-Echeverria C. Antibody-drug conjugates - A new

wave of cancer drugs. *Bioorganic Med Chem Lett*. 2014;24:5357-5363.

41. Shim H. One target, different effects: A comparison of distinct therapeutic antibodies against the same targets. *Exp Mol Med*. 2011;43:539-549.

42. Singh V, Gupta D, Arora R, Tripathi RP, Almasan A, Macklis RM. Surface levels of CD20 determine anti-CD20 antibodies mediated cell death in vitro. *PLoS One*. 2014;9: e111113.

43. U.S. Food and Drug Administration. Zevalin Label. https://www.accessdata.fda.gov/drugsatfda_docs/label/2009/125019s0156.pdf (accessed September 29, 2020).

44. Blakkisrud J, Løndalen A, Holte H, et al. Pre-dosing with lilotomab prior to therapy with 177Lu-lilotomab satetraxetan significantly increases the ratio of tumor to red marrow absorbed dose in non-Hodgkin lymphoma patients. *Eur J Nucl Med Mol Imaging*. 2018;45:1233-1241.